Susceptibilities with multi-quark interactions in PNJL model

Abhijit Bhattacharyya* and Paramita Deb†
Department of Physics, University of Calcutta,
92, A. P. C. Road, Kolkata - 700009, INDIA

Anirban Lahiri‡ and Rajarshi Ray§
Center for Astroparticle Physics & Space Science,
Bose Institute, Block-EN, Sector-V,
Salt Lake, Kolkata-700091, INDIA
&
Department of Physics, Bose Institute,
93/1, A. P. C Road,
Kolkata - 700009, INDIA

We have investigated the fluctuations and the higher order susceptibilities of quark number, isospin number, electric charge and strangeness at vanishing chemical potential for 2+1 flavor Polyakov loop extended Nambu–Jona-Lasinio model. The calculations are performed for the bound effective potential in the quark sector requiring up to eight quark interaction terms. These have been contrasted to the lattice results which currently have somewhat heavier quarks in the light flavor sector. The results show sufficient qualitative agreement. For comparison we also present the results obtained with the conventional effective potential containing upto six quark interaction terms.

PACS numbers: 12.38.Aw, 12.38.Mh, 12.39.-x

I. INTRODUCTION

Confinement and chiral symmetry breaking are the most fundamental properties of strong interaction physics at low temperature and density, where the physics is mainly governed by the non-perturbative QCD. In principle, the deconfinement phase transition and chiral phase transition are defined in two extreme limits of current quark mass. Deconfinement phase transition and its order parameter is well defined for infinite current quark mass and chiral phase transition is exact for zero quark mass. But in real world with a finite value of quark masses, the nature of these two phase transitions is an open question. Another important feature of the QCD phase diagram is the existence of the critical end point (CEP), where first order phase transition, from hadronic phase to quark-gluon-plasma (QGP) phase, ends. However, the exact location of CEP is still unknown. Investigation of these properties of strongly interacting matter are necessary to understand the various astrophysical and cosmological scenario.

The experimental explorations to understand the properties of strongly interacting matter has been studied at Relativistic Heavy-ion-collider (RHIC), Brookhaven [1] where the heavy nuclei collide with each other at relativistic energies to form hot and dense strongly interacting

*Electronic address: abphy@caluniv.ac.in
†Electronic address: paramita.deb83@gmail.com
‡Electronic address: anirbanlahiri.boseinst@gmail.com
§Electronic address: rajarshi@bosemain.boseinst.ac.in

matter. More data are expected from LHC and FAIR in future. But to analyze the data from the experiment, we need a thorough understanding of the theory of strong interaction physics.

Due to our limited knowledge of the non-perturbative physics, QCD, which is the theory of strong interaction, can not be used to study the phase transition picture. In this regard Lattice QCD (LQCD) provides the most direct approach to study QCD at high temperature [2–15]. However LQCD has its own restrictions due to the discretization of space-time. Furthermore, at finite chemical potential, LQCD faces the well known sign problem.

Another approach to study low energy limit of QCD and the QCD phase transition is to use effective theories of QCD. Polyakov loop extended Nambu–Jona-Lasinio model (PNJL) is one of the successful approach which combines the confinement and chiral symmetry breaking properties in a simple formalism. There have been series of work to study the thermodynamic properties of strongly interacting matter using PNJL model for both 2 flavor and 2+1 flavor [16–24]. These studies suggest that this model reproduces the zero density lattice data quite successfully. However, the vacuum of the NJL part of the PNJL model seems to to be unbound in a 2+1 flavor scenario. A plausible solution of this problem has been proposed by Osipov *et.al* using eight-quark interaction term [25–28]. Also the 2 flavor PNJL model have been studied in Ref. [29, 30] with eight-quark interaction. In our previous work, we developed 2+1 flavor PNJL model with eight-quark interaction terms in the Lagrangian with three-momentum cutoff regularisation [31].

The thermodynamic aspect of the phase transition from hadronic phase to QGP phase can be understood properly if we study the thermodynamic variables like quark number susceptibility (QNS), isospin number susceptibility (INS), specific heat (C_V) and speed of sound (v_s) etc. Susceptibilities are related to fluctuations via the fluctuation-dissipation theorem. A measure of the intrinsic statistical fluctuations in a system close to thermal equilibrium is provided by the corresponding susceptibilities. At zero chemical potential, charge fluctuations are sensitive indicators of the transition from hadronic matter to QGP. Also the existence of the CEP can be signalled by the divergent fluctuations. For the small net baryon number, which can be met at different experiments, the transition from hadronic to QGP phase is continuous and the fluctuations are not expected to lead any singular behavior. Recently, the computations on the lattice have been performed for many of these susceptibilities at zero chemical potentials [32–35]. It was shown that at vanishing chemical potential the susceptibilities rise rapidly around the continuous crossover transition region.

The study of higher order moments of fluctuations are also necessary to locate the transition point more accurately. In 2 flavor QCD, it has been shown that the quark number and isospin number fluctuations increase with temperature and their fourth moments start to show pronounced peaks in the transition region from low to high temperature [8, 36]. In fact the higher order coefficients become increasingly sensitive in the vicinity of phase transition. Fluctuations are computed with respect to the quark chemical potential in 2 flavor PNJL model with three-momentum cutoff regularisation [22, 37–39]. Also QNS at finite density has been estimated in some works within 2 flavor PNJL model [40]. Recently the idea of the Taylor expansion in terms of chemical potential for PNJL model has been computed within the constraint that the net strange quark density is zero, which is the case in ultra relativistic heavy ion collision [41]. There have been recent calculations towards the fluctuations in 2+1 flavor Lattice QCD [42–44] and also in the 2+1 flavor PNJL model taking upto six-quark determinant interaction terms [19, 45]. Similar calculations have been carried out in Polyakov loop coupled quark-meson (PQM) model [46–49] and its renormalization group improved version [50].

In this paper we have investigated the susceptibilities within 2+1 flavor PNJL model framework with two different kinds of NJL interaction. In one case we take the conventional form which takes into account upto six-quark determinant interaction, which we will call as model A.

In the other case an extra eight-quark interaction term is added to make the effective potential bound, which will be hereafter denoted by model B. We have also studied the specific heat and the speed of sound. Specific heat is related to the event-by-event temperature fluctuations [51] and mean transverse momentum fluctuations [52] in heavy-ion reactions. These fluctuations show diverging behavior near the critical end point (CEP). The speed of sound determines the flow properties in heavy-ion reactions [53, 54].

Our paper is organized as follows: In Sec. II, the basic formalism of the PNJL model and also the calculation of fluctuations have been discussed. Various thermodynamic quantities such as specific heat, speed of sound are also defined in this section. In the next section we describe our results and compared with the recent lattice data and also with other models like Polyakov extended quark-meson model (PQM). In the last section we conclude.

II. FORMALISM

A. Thermodynamic Potential

The PNJL model was formulated to study the chiral properties and the confinement physics of the QCD phase transition at finite temperature and density. In this model quark dynamics is studied with a background gauge field having only the temporal component. For a detailed review of the PNJL model with 2 flavor and 2+1 flavor see Ref. [16, 19, 21, 22, 24, 37–41, 45, 50]. Osipov *et.al* pointed out that the effective potential of the NJL part is seems to be unbound in the conventional form and they have introduced the eight-quark interaction terms in NJL model to stabilize the vacuum [25–28]. Also the 2 flavor PNJL model have been studied in Ref. [29, 30] with eight-quark interaction. In our previous paper we developed the 2+1 PNJL model with eight-quark interactions within three-momentum cutoff scheme [31] for the first time. We have reproduced the thermodynamic properties of QCD, calculated on Lattice, at zero baryon density quite satisfactorily. The thermodynamic potential for the multi-fermion interaction in the mean field approximation (MFA) of the PNJL model can be written as [31],

$$\begin{aligned}\Omega =& \mathcal{U}'[\Phi,\bar{\Phi},T] + 2g_S\sum_{f=u,d,s}\sigma_f^2 - \frac{g_D}{2}\sigma_u\sigma_d\sigma_s + 3\frac{g_1}{2}(\sum_{f=u,d,s}{\sigma_f}^2)^2 \\ &+ 3g_2\sum_{f=u,d,s}\sigma_f^4 - 6\sum_{f=u,d,s}\int_0^\Lambda\frac{d^3p}{(2\pi)^3}E_f\Theta(\Lambda-|\vec{p}|) \\ &- 2T\sum_{f=u,d,s}\int_0^\infty\frac{d^3p}{(2\pi)^3}\ln\left[1+3(\Phi+\bar{\Phi}e^{-\frac{(E_f-\mu_f)}{T}})e^{-\frac{(E_f-\mu_f)}{T}}+e^{-3\frac{(E_f-\mu_f)}{T}}\right] \\ &- 2T\sum_{f=u,d,s}\int_0^\infty\frac{d^3p}{(2\pi)^3}\ln\left[1+3(\bar{\Phi}+\Phi e^{-\frac{(E_f+\mu_f)}{T}})e^{-\frac{(E_f+\mu_f)}{T}}+e^{-3\frac{(E_f+\mu_f)}{T}}\right] \end{aligned} \quad (1)$$

g_S and g_D are the four-quark and six-quark coupling constants respectively and g_1 and g_2 are the eight-quark coupling constants. Here $\sigma_f = \langle\bar{\psi}_f\psi_f\rangle$ denotes chiral condensate of the quark with flavor f and $E_f = \sqrt{p^2+M_f^2}$ is the single quasi-particle energy. Here, constituent mass M_f of flavor f is given by the self-consistent gap equation;

$$M_f = m_f - 2g_S\sigma_f + \frac{g_D}{2}\sigma_{f+1}\sigma_{f+2} - 2g_1\sigma_f(\sigma_u^2+\sigma_d^2+\sigma_s^2) - 4g_2\sigma_f^3$$

where f, $f+1$ and $f+2$ take the labels of flavor u, d and s in cyclic order. So, when $f = u$ then $f + 1 = d$ and $f + 2 = s$ and so on. In the above integrals, the vacuum integral has a cutoff Λ whereas the medium dependent integrals have been extended to infinity. Polyakov loop being the normalized trace of the Wilson line $\mathbf{L}$, which is an SU(3) matrix, should lie in the range $0\leqslant \Phi \leqslant 1$. But earlier studies of PNJL model [22, 24, 39] show that the Φ becomes greater than 1 above $2T_C$. To solve this problem one has to take a proper Jacobian of transformation from the matrix valued field $\mathbf{L}$ to the complex valued field Φ. This will constrain the value of Φ within 1. Thus one has to modify the Polyakov loop potential by introducing Vandermonde (VdM) term. The necessity of the modification was reflected through an excellent agreement of flavour mixing effects in PNJL model with lattice data as shown in Ref. [23]. There are a few extra terms in $\mathcal{U}(\Phi, \bar{\Phi})$ in this prescription as compared to other recent works [19, 37]. These extra terms are put on the basis of the global Z(3) symmetry of the Polyakov loop potential and therefore their presence seem to be quite natural though may not be absolutely necessary as shown by [19, 37]. The modified potential $\mathcal{U}'$ can be expressed as ,

$$\frac{\mathcal{U}'(\Phi, \bar{\Phi}, T)}{T^4} = \frac{\mathcal{U}(\Phi, \bar{\Phi}, T)}{T^4} - \kappa \ln[J(\Phi, \bar{\Phi})] \tag{2}$$

where $\mathcal{U}(\Phi, \bar{\Phi}, T)$ is the Landau-Ginzburg type potential given by [17],

$$\frac{\mathcal{U}(\Phi, \bar{\Phi}, T)}{T^4} = -\frac{b_2(T)}{2}\bar{\Phi}\Phi - \frac{b_3}{6}(\Phi^3 + \bar{\Phi}^3) + \frac{b_4}{4}(\bar{\Phi}\Phi)^2 \tag{3}$$

with,

$$b_2(T) = a_0 + a_1(\frac{T_0}{T}) + a_2(\frac{T_0}{T})^2 + a_3(\frac{T_0}{T})^3, \tag{4}$$

and b_3, b_4 being constants. $J(\Phi, \bar{\Phi})$ in eqn. (2) is known as VdM determinant [23], is given by,

$$J[\Phi, \bar{\Phi}] = (27/24\pi^2)(1 - 6\Phi\bar{\Phi} + 4(\Phi^3 + \bar{\Phi}^3) - 3(\Phi\bar{\Phi})^2)$$

κ is a phenomenological constant. Polyakov loop Φ and its charge conjugate $\bar{\Phi}$ is defined as,

$$\Phi = (\mathrm{Tr_c L})/\mathrm{N_c}, \qquad \bar{\Phi} = (\mathrm{Tr_c L^\dagger})/\mathrm{N_c}$$

The parameter T_0 is taken as 190 MeV, whereas the lattice determines its value to be 270 MeV for pure gauge theory. The reason to take a lower value of T_0 is to get the crossover temperature (T_c) consistent with the lattice data. In this work we have taken the parameter set obtained in our previous paper [31]. For fixing the parameters $m_s, \Lambda, g_S, g_D, g_1, g_2$ we have used the following physical conditions;

$m_\pi = 138\,\mathrm{MeV}$ $f_\pi = 93\,\mathrm{MeV}$ $m_K = 494\,\mathrm{MeV}$ $f_K = 117\,\mathrm{MeV}$ $m_\eta = 480\,\mathrm{MeV}$ $m_{\eta'} = 957\,\mathrm{MeV}$

and m_u is kept fixed at 5.5 MeV. The parameters are given in table I for both PNJL model A and PNJL model B.

For the Polyakov loop potential we choose the parameters which reproduces the lattice data of pure gauge thermodynamics [55]. It was shown in Ref. [17] that, pure gauge Lattice QCD data of scaled pressure, entropy and energy density are reproduced extremely well in Polyakov loop model using the ansatz (3) and (4) with parameters summarized below,

$$a_0 = 6.75, a_1 = -1.95, a_2 = 2.625, a_3 = -7.44, b_3 = 0.75, b_4 = 7.5$$

Interaction	m_u (MeV)	m_s (MeV)	Λ (MeV)	$g_S\Lambda^2$	$g_D\Lambda^5$	$g_1 \times 10^{-21}$ (MeV^{-8})	$g_2 \times 10^{-22}$ (MeV^{-8})	κ	T_C (MeV)
ModelA	5.5	134.758	631.357	3.664	74.636	0.0	0.0	0.13	181
ModelB	5.5	183.468	637.720	2.914	75.968	2.193	−5.890	0.06	169

TABLE I: Parameters and T_C for model A and model B Lagrangians.

B. Taylor expansion of pressure

The pressure of the strongly interacting matter can be written as,

$$P(T, \mu_q, \mu_Q, \mu_S) = -\Omega(T, \mu_q, \mu_Q, \mu_S), \tag{5}$$

where T is the temperature, μ_q is the quark chemical potential, μ_Q is the charge chemical potential and μ_S is the strangeness chemical potential. From the usual thermodynamic relations we can show that the first derivative of pressure with respect to μ_q gives the quark number density and the second derivative is the quark number susceptibility (QNS).

Our first job is to minimize the thermodynamic potential numerically with respect to the fields σ_u, σ_d, σ_s, Φ and $\bar{\Phi}$. The values of the fields can then be used to evaluate the pressure using the equation (5). Then we can expand the scaled pressure at a given temperature in a Taylor series for the chemical potentials μ_q, μ_Q, μ_S as,

$$\frac{p(T, \mu_q, \mu_Q, \mu_S)}{T^4} = \sum_{i,j,k} c^{q,Q,S}_{i,j,k} (\frac{\mu_q}{T})^i (\frac{\mu_Q}{T})^j (\frac{\mu_S}{T})^k \tag{6}$$

where,

$$c^{q,Q,S}_{i,j,k}(T) = \frac{1}{i!j!k!} \frac{\partial^i}{\partial(\frac{\mu_q}{T})^i} \frac{\partial^j}{\partial(\frac{\mu_Q}{T})^j} \frac{\partial^k (P/T^4)}{\partial(\frac{\mu_S}{T})^k}\Big|_{\mu_{q,Q,S}=0} \tag{7}$$

The flavor chemical potentials μ_u, μ_d, μ_s are related to μ_q, μ_Q, μ_S by,

$$\mu_u = \mu_q + \frac{2}{3}\mu_Q, \quad \mu_d = \mu_q - \frac{1}{3}\mu_Q, \quad \mu_s = \mu_q - \frac{1}{3}\mu_Q - \mu_S \tag{8}$$

It should be mentioned that one can also choose the independent chemical potentials as μ_q, μ_I, μ_S. Then eqn.(8) becomes,

$$\mu_u = \mu_q + \mu_I, \quad \mu_d = \mu_q - \mu_I, \quad \mu_s = \mu_q - \mu_S \tag{9}$$

where, μ_I is the isospin chemical potential. Eq.(6) is a general expression of Taylor expansion of pressure for different chemical potentials. Since in this paper we are only concerned with the diagonal terms of the expansion, we can write the above equation in simpler way as,

$$\frac{p(T, \mu_X)}{T^4} = \sum_{n=0}^{\infty} c^X_n(T) (\frac{\mu_X}{T})^n \tag{10}$$

where,

$$c^X_n(T) = \frac{1}{n!} \frac{\partial^n (P(T, \mu_X)/T^4)}{\partial(\frac{\mu_X}{T})^n}\Big|_{\mu_X=0} \tag{11}$$

Where X is q, Q or I and S. Here we will use the expansion around $\mu_X = 0$, where the odd terms vanish due to CP symmetry. In this work we evaluate the expansion coefficients up to eighth order. To obtain the Taylor coefficients, first the pressure is obtained as a function of μ_X for each value of T, then fitted to a polynomial about $\mu_X = 0$. All orders of derivatives are then obtained from the coefficients of the polynomial extracted from the fit. For the stability of the fit we have checked the values of least squares.

C. Specific heat and speed of sound

We have studied the specific heat C_V, which is important to find the location of CEP, the speed of sound, which determines the flow properties in heavy-ion reactions. The energy density ϵ is obtained from the thermodynamic potential Ω as,

$$\epsilon = -T^2 \frac{\partial(\Omega/T)}{\partial T}\Big|_V = -T\frac{\partial\Omega}{\partial T}\Big|_V + \Omega$$

The specific heat is defined as the rate of change of energy density with temperature at constant volume, which is given by,

$$C_V = \frac{\partial\epsilon}{\partial T}\Big|_V = -T\frac{\partial^2\Omega}{\partial T^2}\Big|_V.$$

For a continuous phase transition near CEP, it is expected that C_V shows a diverging behavior, which will translate into highly enhanced transverse momentum fluctuations or highly suppressed temperature fluctuations. The square of speed of sound at constant entropy S is given by,

$$v_s^2 = \frac{\partial P}{\partial\epsilon}\Big|_S = \frac{\partial P}{\partial T}\Big|_V \Big/ \frac{\partial\epsilon}{\partial T}\Big|_V = \frac{\partial\Omega}{\partial T}\Big|_V \Big/ T\frac{\partial^2\Omega}{\partial T^2}\Big|_V \quad . \tag{12}$$

Divergence in specific heat near CEP means vanishing speed of sound.

III. RESULT

We now present the coefficients of the Taylor expansion of pressure for 2+1 flavor PNJL model with model A and model B Lagrangians and make a comparative study between the quark number susceptibility (QNS), isospin number susceptibility (INS), charge and strangeness susceptibility and their higher order derivatives. We then compare the specific heat and the speed of sound for both Lagrangians. We also compare our results with the recent lattice data available for 2+1 flavor with $N_\tau = 6$ [43] and also with that of Polyakov extended quark-meson model (PQM) [46–49].

A. Coefficients of the Taylor expansion

The pressure is fitted to a polynomial in μ_X using the "gnuplot"[57] program at different values of temperature. Here we consider to take maximum eighth order term in the polynomial in μ_X. We restrict our expansion range to $\mu_q \sim 300$ MeV above which the diquark physics is expected to become important. Also the pion condensation and kaon condensation takes place in NJL model for $\mu_I > 70$ MeV and $\mu_S > 240$ MeV respectively. So we restrict our range within

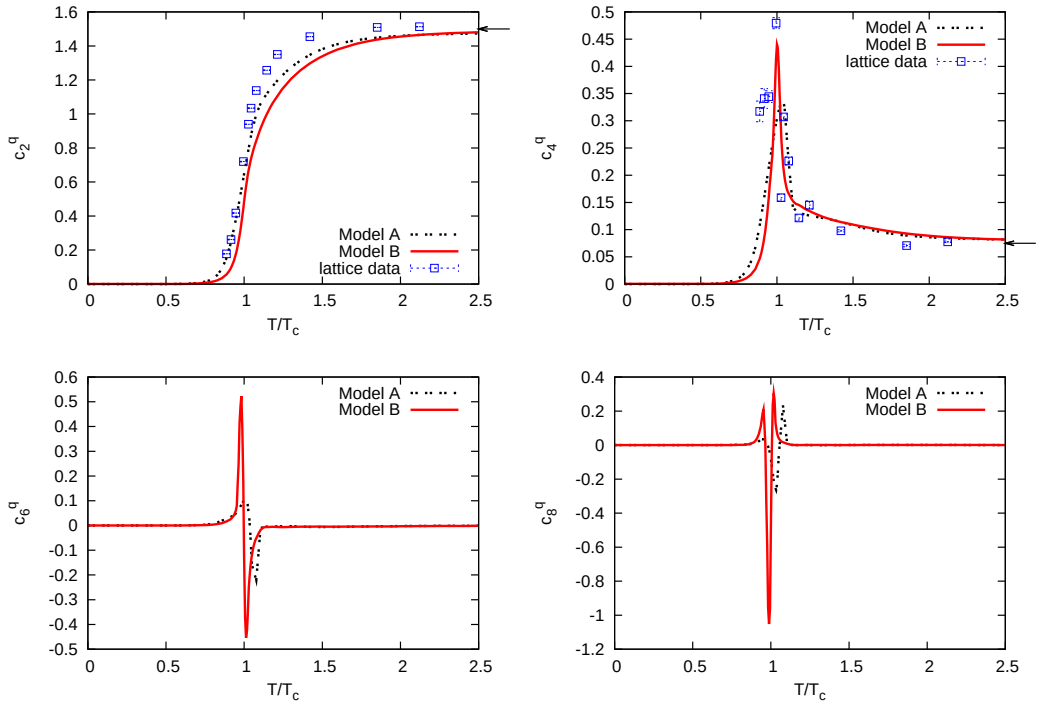

FIG. 1: (color online). Variation of c_2, c_4, c_6 and c_8 with T/T_C, for $\mu_X = \mu_q$ for models A and B. The arrows on the right show the corresponding SB limits. The lattice are data taken from Ref. [43].

$\mu_I < 70$ MeV and $\mu_S < 200$ MeV below T_C. However, above T_C, approximate restoration of chiral symmetry implies that the chiral condensates become almost zero. So above T_C, we have extended the range of μ_I and μ_S for the better fit of the coefficients. Near T_C the χ^2 (which is same as the least square here) of the fit varies rapidly with the variation of range of μ_X over which the fit was done. So near T_C we have fitted the pressure for 1 MeV gap of temperature and the data points are spaced by 0.1 MeV of chemical potential for all temperature values. The least-squares of all the fits came out to be 10^{-10} or less.

Now we study the behavior of the coefficients c_2, c_4, c_6 and c_8 for three sets of chemical potentials for model A and model B. In figure (1) we show the variation of c_2, c_4, c_6 and c_8 with T/T_C for $\mu_X = \mu_q$ for both models and lattice data. It can be seen that QNS (c_2^q) shows an order parameter like behavior. At low temperature there are small differences between model A and model B and model A is much closer to the lattice data. At high temperature c_2^q for model A reaches almost 98% of its ideal gas value whereas for model B it reaches almost 99% of its ideal gas value. However lattice data for $N_\tau = 6$ at high temperature reaches almost the Stefan-Boltzmann (SB) limit. The fourth order derivative c_4^q can be thought of as the susceptibility of c_2^q. The figure shows a peak near T_C. Near T_C the model B shows much higher peak than the model A and the peak of the eight-quark interaction is closer to the lattice data. At higher temperature both cases match very well with the lattice data. But near and above $2T_C$ lattice value converges to the SB limit, however both cases of PNJL model are slightly away from the SB limit. Note that both c_2^q and c_4^q have only fermionic contribution in the

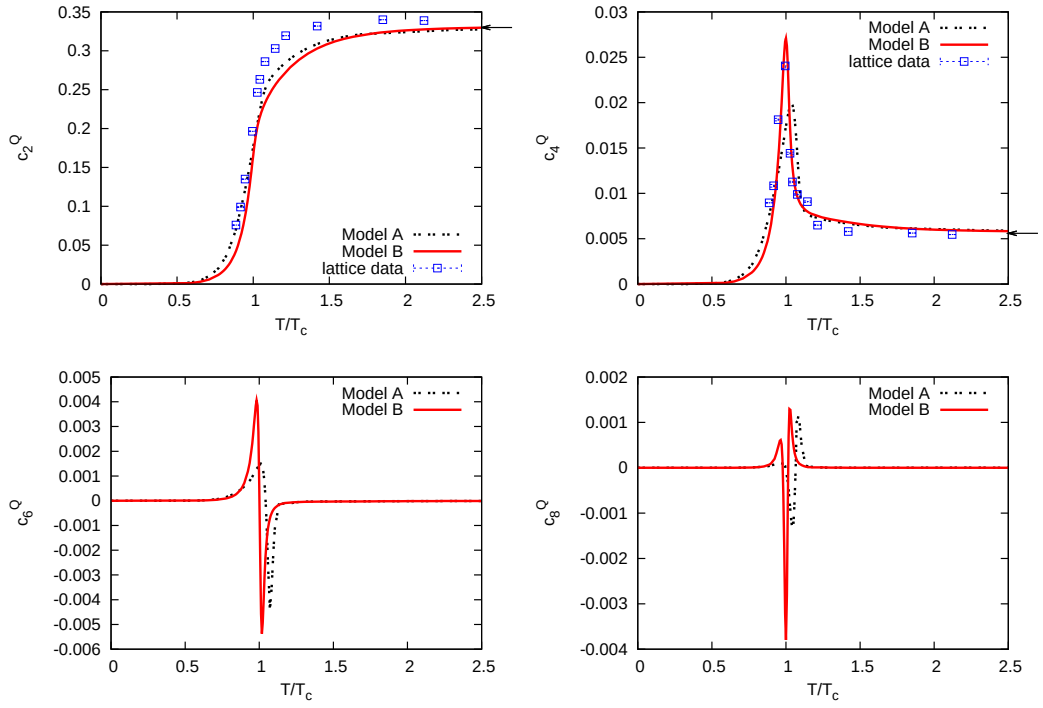

FIG. 2: (color online). Variation of c_2, c_4, c_6 and c_8 with T/T_C, for $\mu_X = \mu_Q$ for models A and B. The arrows on the right show the corresponding SB limits. The lattice data are taken from Ref. [43].

SB limit. Since, the coupling strength is large enough for $T < 2.5T_C$, a sufficient amount of interaction is present in the system. So, it is expected that c_4^q will not converge exactly to the SB limit within $T < 2.5T_C$. The higher order coefficients c_6^q and c_8^q show interesting behavior near T_C. Although at very low and high temperatures both of them converge to zero. Near T_C, c_6^q shows sharp peaks for both cases. However for model B the peak is much sharper. Similar behavior can be observed for c_8^q, which shows more peaks near T_C. The reason behind the peaks near the transition temperature may be due to the increase in fluctuation near T_C. The sharper peaks of model B is probably due to the introduction of enhanced repulsive interaction through eight-quark term. This was also reflected through the increase of scaled pressure in case of model B Lagrangian over the model A [31]. The number of peaks increases near T_C for higher order coefficients. In figure (2) the variation of susceptibility and the higher order coefficients for the charge chemical potential is shown. The nature of all the coefficients are same as the quark chemical potential. At high temperature the fluctuation c_2^Q for model B is closer to the SB limit compared to the model A. However lattice data is slightly above the SB limit for c_2^Q. For the case of c_4^Q, our data (for both cases) show a better convergence towards SB limit, unlike c_4^q. At low temperature the behavior of model A is closer to the lattice data compared to the model B. The quartic fluctuations show a peak near T_C. The peak for model B is sharper than model A and the plot for model B matches well with the lattice result. The higher order coefficients show similar behavior as the quark chemical potential case.

The figure (3) shows the variation of susceptibility and the higher order coefficients for the

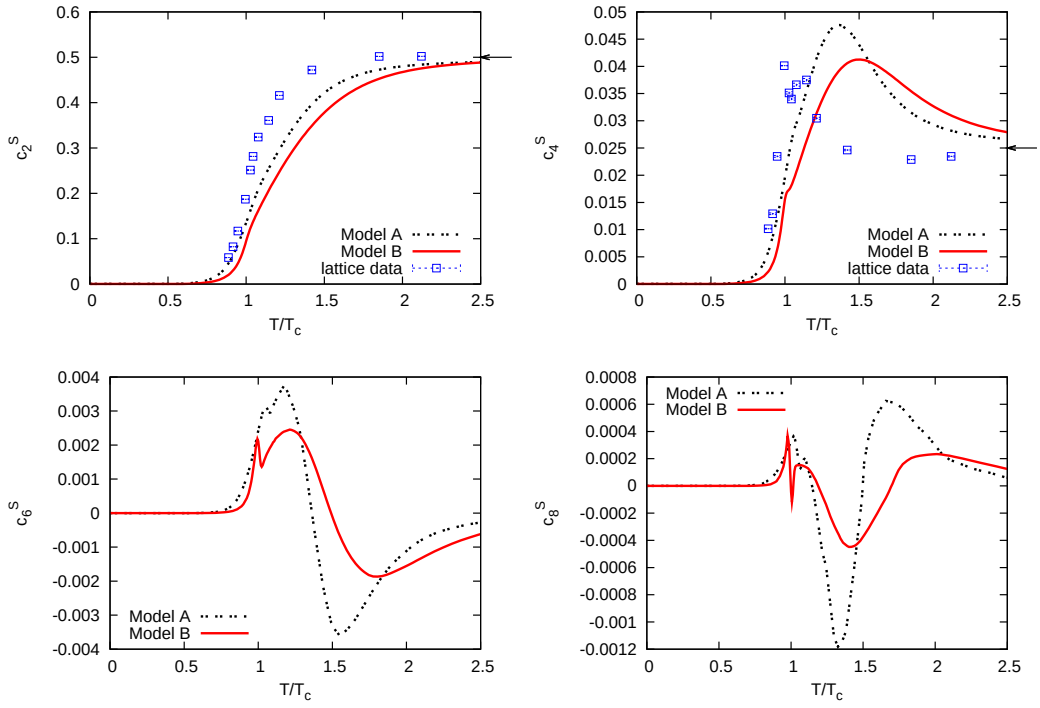

FIG. 3: (color online). Variation of c_2, c_4, c_6 and c_8 with T/T_C, for $\mu_X = \mu_S$ for models A and B. The arrows on the right show the corresponding SB limits. The lattice are data taken from Ref. [43].

strangeness chemical potential with T/T_C. The c_2^S for both the models are slightly different from the lattice data. Both the plots are almost 98% of the SB limit at high temperature, however the lattice data coincides with the SB limit. The c_4^S has a similar behavior as the c_4^q. However the peak is not near T_C in this case. Near T_C we can see a small bump for both type of Lagrangian, but the peak in both case is at higher temperature. This is due to the fact that during the chiral crossover the strange quark (the only element which carries strangeness) is sufficiently heavy and the corresponding condensate σ_s melts at much higher temperature than T_C. The maxima of $d\sigma_s/dT$ and c_4^S coincide at the temperature where peaks are observed. This behavior is quite consistent with the lattice results which also indicates two peaks. However in case of lattice, the peak at T_C is higher than the second peak. So, one can not really pin down the cause of the double peak structure. It may be a model artifact. At high temperature both the curves are above the SB limit. But the lattice data is slightly below the SB limit. The higher order derivatives also show a sharp peak at the transition temperature followed by a broader peak at higher temperature for both model A and Model B.

For the sake of completeness we have also plotted different moments of pressure for isospin chemical potential μ_I in fig. (4). It is clearly seen that, c_2^I has also an order parameter like behavior like all other susceptibilities both models. At high temperature, the plot for model B reaches almost 99.5% of the SB limit, whereas the plot for model A reaches close to 98% . For c_4^I, the plot for the model B shows higher peak than the case of model A at T_C and both of them converges very well towards the SB limit at high temperature. The c_6^I and c_8^I shows very

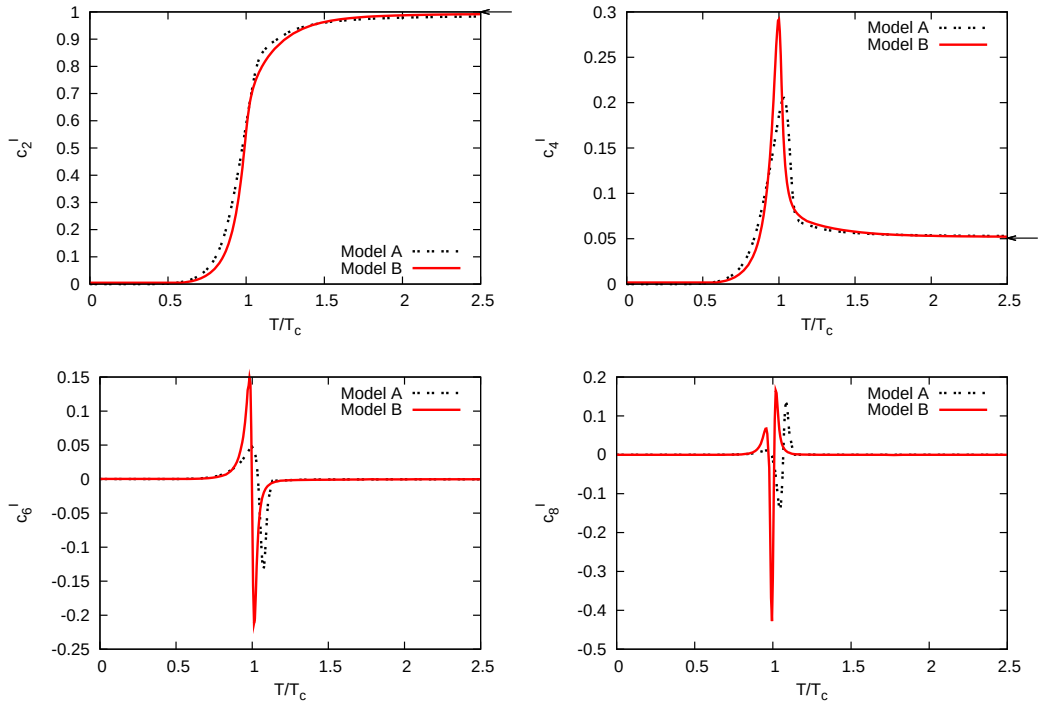

FIG. 4: (color online). Variation of c_2, c_4, c_6 and c_8 with T/T_C, for $\mu_X = \mu_I$ for models A and B. The arrows on the right show the corresponding SB limits. The lattice data are taken from Ref. [43].

rapidly fluctuating peak structure near T_C and goes to zero in both high and low temperature regime.

In figure (5) we show a comparative study for c_2, c_4, c_6 and c_8 with T/T_C for μ_q, μ_I, μ_S and μ_Q for both type of Lagrangian. In all cases we can see that the quadratic fluctuations rise rapidly in the transition region where the quartic fluctuations show a peak. This peak is most pronounced in case of μ_q. The generic form of this temperature dependence, a smooth crossover for quadratic fluctuations and a peak in quartic fluctuations, is in fact expected to occur in the vicinity of the chiral phase transition of QCD. For all of the coefficients the fluctuation in μ_q direction is strongest followed by the isospin direction fluctuations and the strangeness fluctuation. The charge fluctuation is the least pronounced. The quartic fluctuation for μ_S shows a peak at much higher temperature than the transition temperature. However other three c_4^q, c_4^Q and c_4^I show peaks at T_C. For higher order coefficients the strangeness and charge fluctuations are negligible near T_C compared to the quark number and isospin fluctuations.

In fig (6) we have plotted the kurtosis *i.e.* the ratio of c_4^X/c_2^X for both type of potential (where $X = q, Q$ or S) and compared with the lattice data. The plot for c_4^q/c_2^q for model B shows more fluctuation near T_C than model A. However lattice data shows higher fluctuation near T_C than the model study. At higher temperature both models coincide with the lattice data and converges well with the SB limit. Our results are qualitatively similar with PQM result [48]. In case of the ratio c_4^Q/c_2^Q the model B shows more fluctuation than the model A and as well as the lattice data. The model B shows almost 99% convergence with the SB limit

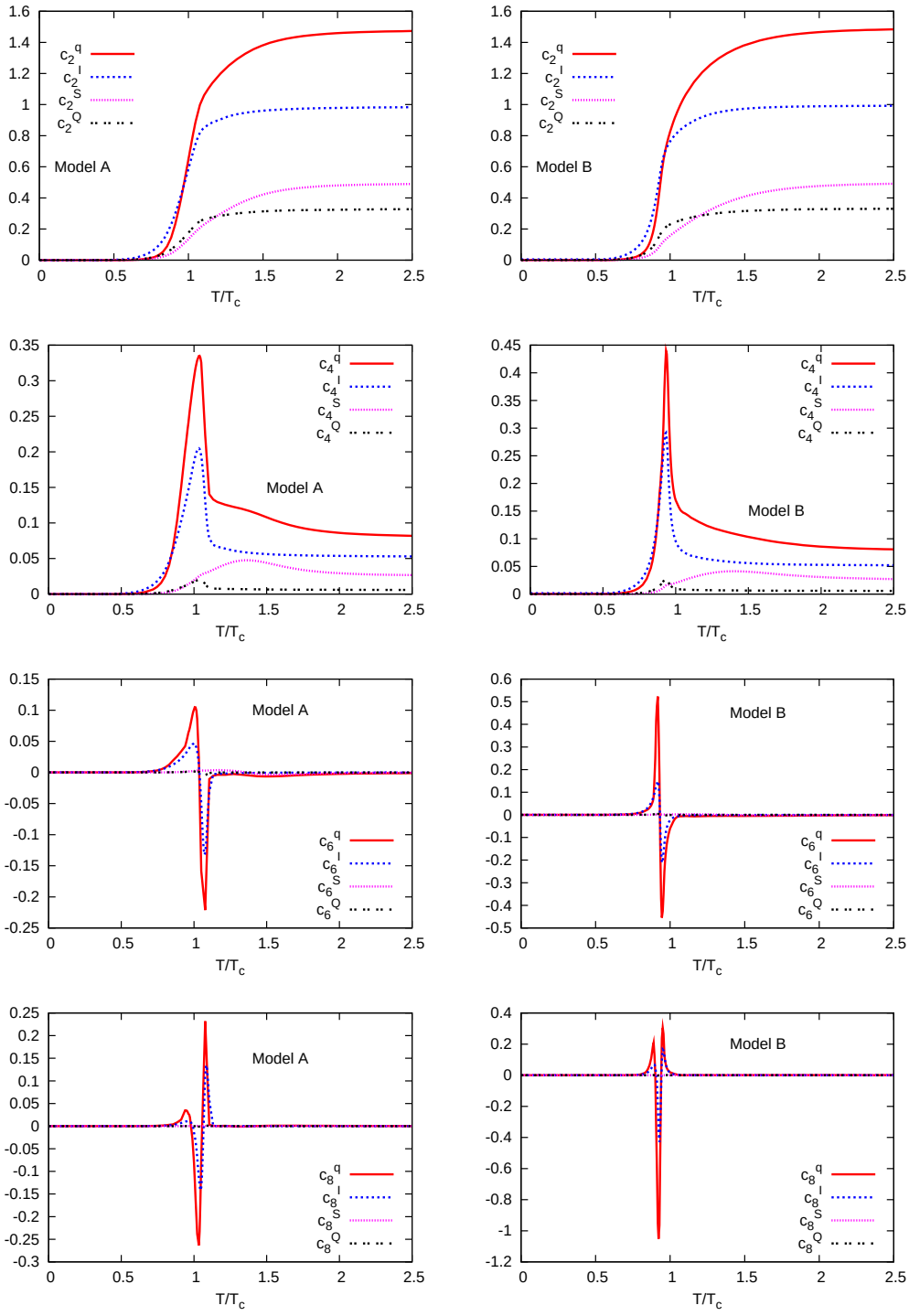

FIG. 5: (color online). Comparative study of c_2^X, c_4^X, c_6^X and c_8^X for models A and B, where X=q, Q, I or S.

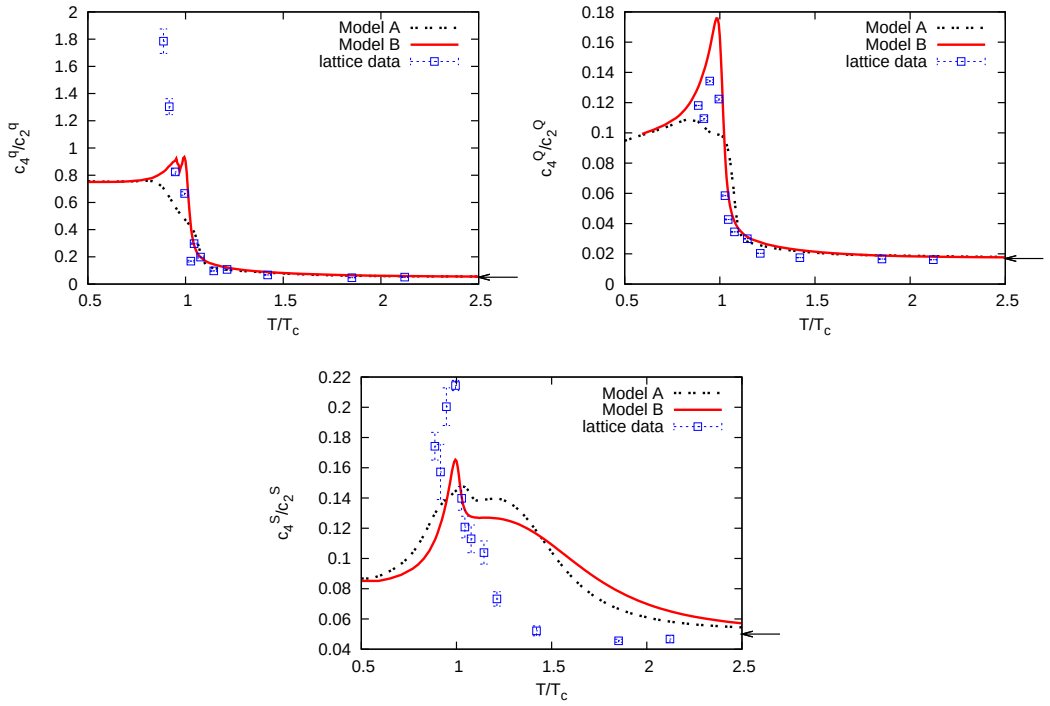

FIG. 6: (color online). Variation of c_4/c_2 with T/T_C, for μ_q, μ_Q and μ_S for models A and B. The arrows on the right show the corresponding SB limits. The lattice data are taken from Ref. [43]. The upper left panel corresponds to the quark chemical potential, the upper right panel corresponds to the charge chemical potential and the lower panel corresponds to the strangeness chemical potential

at high temperature. For the strangeness fluctuation, we can see two peaks in c_4^S/c_2^S curve for the both models. First peak occurs at chiral transition for light flavors and second peak occurs when chiral transition occurs in strange sector. At intermediate temperatures PNJL model overestimates the ratio than LQCD result. This feature is also observed in PQM model [48]. In PQM model the ratio approaches the SB limit at high temperature and near the transition region sharp peaks appear. In our case the ratio shows sharper peak near the transition temperature and a broader peak at a higher temperature than T_C. However lattice data shows much higher fluctuations than the plots for both models near T_C. At high temperature the model A is closer to the SB limit than the model B.

B. Specific heat and the speed of sound

We now discuss the thermodynamic quantities like specific heat (C_V) and the speed of sound (v_s). In Fig. (7) we have plotted C_V/T^3 with T/T_C for both models. From the plot we can see that C_V grows with increasing temperature and reaches a peak at T_C for both models. However model B shows a sharper peak at T_C compared to the model A. Just above T_C both the plots decrease sharply for a short range of temperature. Thereafter it gradually converges to a value slightly lower than the ideal gas value at high temperature. However the convergence towards the ideal gas value is better in case of model B. For comparison we have also plotted the values

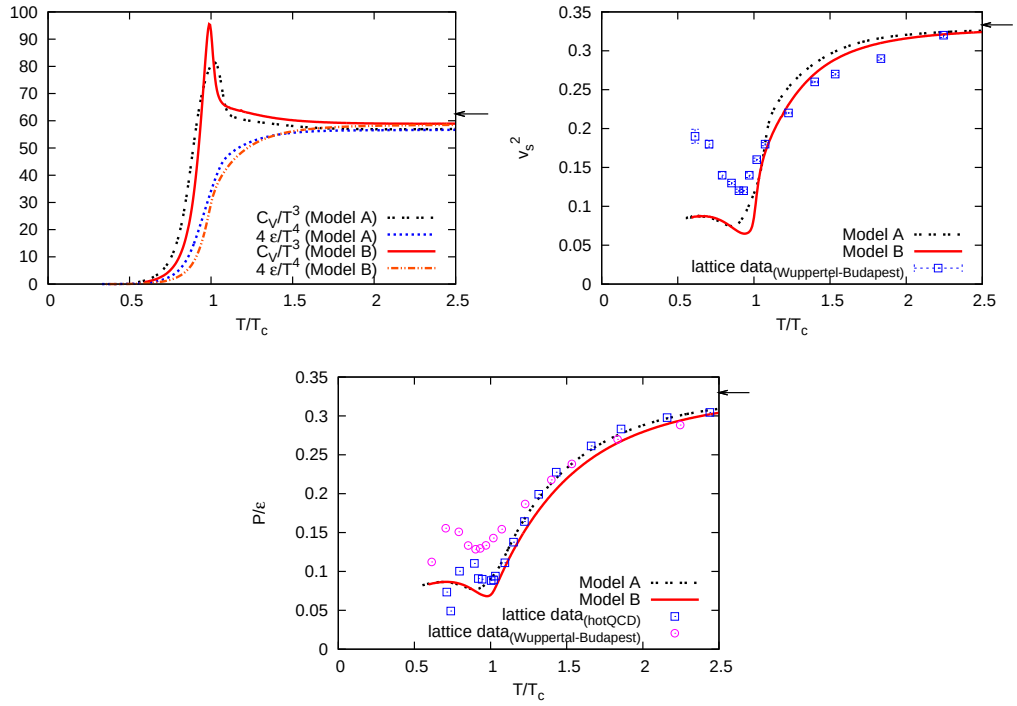

FIG. 7: (color online). Variation of C_V/T^3, $4\epsilon/T^4$, v_s^2 and p/ϵ with T/T_C, for models A and B. The arrows on the right show the corresponding SB limits. The upper left panel shows the plot for C_V/T^3 and $4\epsilon/T^4$ with T/T_C, the upper right panel shows the comparison of v_s^2 for models A and B and the lattice data given by [44] and the bottom panel shows the comparison of p/ϵ of both models and the lattice data given by [42, 44]

of $4\epsilon/T^4$, at which the specific heat is expected to coincide for a conformal gas. From the graph we can see that the specific heat converges very well with the $4\epsilon/T^4$ at high temperature for both the models. Both the plots of C_V/T^3 and $4\epsilon/T^4$ show similar behavior as PQM model [48]. In PQM model C_V grows with temperature and shows a sharp peak at T_C. After the peak a broad bump is found around $1.2T_C$ and then C_V goes gradually to the ideal gas value.

We now consider the speed of sound and p/ϵ for model A and model B in figure (7). We can see that v_s^2 is slightly below the ideal gas value at temperature $2.5T_C$ for both cases. Our result is quite consistent with the lattice data for 2+1 flavor staggered fermions reported in [56]. A similar behavior as ours is observed in PQM model [48]. We get the minimum of v_s^2 just below the T_C similar to lattice data [56] and the softest point of the equation of state is found to be $(p/\epsilon)_{min} \approx 0.07$ for model A and $(p/\epsilon)_{min} \approx 0.06$ for model B. Model B gives better agreement with lattice data, which has its softest point of equation of state as $(p/\epsilon)_{min} \approx 0.05$. We have compared two sets of lattice data of Ref. [42] and Ref. [44] with our model study. Our result shows a better agreement with that of Ref. [42]. The softest point of equation of state of [42] is at $(p/\epsilon)_{min} \approx 0.08$, whereas the softest point of Ref. [44] is at much higher value ~ 0.13. In case of PQM model the softest point of the equation of state is found to be around ≈ 0.04 [48] which is closer to our value.

IV. DISCUSSION

We have studied the various fluctuations and some of the thermodynamic quantities using two diferent versions of PNJL model to understand the properties of the strongly interacting matter. In fact it is expected that the susceptibilities and the higher order fluctuations might provide the direct evidence of the order of the QCD phase transition. A pronounced peak in the susceptibility can depict the crossover transition and the sharp diverging behavior would indicate the existence of a phase transition.

We have also obtained the susceptibilities and the higher order derivatives by the Taylor expansion of pressure for two kinds of PNJL model near $\mu_X = 0$, where $X = q, I$ or Q and S. In all cases the second derivative of pressure which is known as the susceptibility, show a steep rise near the transition region, which indicates near the transition region the fluctuation increases. However at higher temperature c_2^X almost saturates and almost converges to the ideal gas value. This result is quite consistent with the lattice data. The higher order fluctuation c_4 shows a peak near T_C for both models and the result matches with the lattice data. The finite height of the peak confirms the crossover nature of transition at $\mu = 0$. Both c_6 and c_8 show rapid variation around T_C for all cases.

We have also calculated the specific heat, speed of sound for both kinds of PNJL model. The plot for C_V/T^3, after showing a peak at T_C, converges very well to $4\epsilon/T^4$ curve at high T. At high temperature v_s^2 almost reaches its ideal gas value $1/3$ and the softest point of the equation of state has a better agreement with lattice result for model B where eight-quark interaction is taken into account.

In our formalism, we do not include pion condensate, kaon condensate and diquark condensate which may play an important role for higher values of chemical potential. Inclusion of those degrees of freedom may improve our result. Involved though, such studies are in progress.

V. ACKNOWLEDGEMENT

P.D. and A.L. would like to thank CSIR for financial support. A.B. thanks CSIR and UGC (UPE and DRS) for support. The authors thank Saumen Datta for some useful discussions.

[1] K. Adcox *et al*, Nucl. Phys. **A 757**, 184 (2005).
[2] G. Boyd, J. Engels, F. karsch, E. Laermann, C. legeland, M. Lugermeier and B. Peterson, Nucl. Phys. **B 469**, 419 (1996).
[3] J. Engels, O. Kaczmarek, F. Karsch, and E. Laermann, Nucl. Phys. **B 558**, 307 (1999).
[4] Z. Fodor, and S. D. Katz, Phys. Lett. **B 534**, 87 (2002).
[5] Z. Fodor, S. D. Katz and K. K. Szabo, Phys. Lett. **B 568**, 73 (2003).
[6] C. R. Allton, S. Ejiri, S. J. Hands, O. Kaczmarek, F. Karsch, E. Laermann, Ch. Schmidt, and L. Scorzato, Phys. Rev. **D 66**, 074507 (2002).
[7] C. R. Allton, S. Ejiri, S. J. Hands, O. Kaczmarek, F. Karsch, E. Laermann, and Ch. Schmidt, Phys. Rev. **D 68**, 014507 (2003).
[8] C. R. Allton, M. Doring, S. Ejiri, S. J. Hands, O. Kaczmarek, F. Karsch, E. Laermann, and K. Redlich, Phys. Rev. **D 71**, 054508 (2005).
[9] P. de Forcrand, and O. Philipsen, Nucl. Phys. **B 642**, 290 (2002); Nucl. Phys. **B 673**, 170 (2003).
[10] Y. Aoki, Z. Fodor, S. D. katz, and K. K. Szabo, Phys. Lett. **B 643**, 46 (2006).
[11] Y. Aoki, G. Endrodi, Z. Fodor, S. D. Katz and K. K. Szabo, Nature **443**, 675 (2006).

[12] E. Megias, E. Ruiz Arriola, L. L. Salcedo, Rom. Rep. Phys. **58**, 081-086, (2006)
[13] E. Megias, E. R. Arriola, L. L. Salcedo, Pos JHW2005, 025, (2006).
[14] E. Megias, E. R. Arriola, L. L. Salcedo, Nucl. Phys. Proc. Suppl. **186**, 256-259, (2009).
[15] E. Megias, E. R. Arriola, L. L. Salcedo, Phys. Rev. **D 81**, 096009, (2010).
[16] K. Fukushima, Phys. Lett. **B 591**, 277 (2004).
[17] C. Ratti, M. A. Thaler and W. Weise, Phys. Rev. **D 73**, 014019 (2006).
[18] R. D. Pisarski, Phys. Rev. **D 62**, 111501 (2000); A. Dumitru and R. D. Pisarski, Phys. lett. **B 504**, 282 (2001), Phys. lett. **B 525**, 95 (2002), Phys. Rev. **D 66**, 096003 (2002).
[19] K. Fukushima, Phys. Rev. **D 77**, 114028, (2008).
[20] H. Hansen, W. M. Alberico, A. Beraudo, A. Molinari, M. Nardi and C. Ratti, Phys. Rev. **D 75**, 065004 (2007).
[21] M. Ciminale, R. Gatto, N. D. Ippolito, G. Nardulli and M. Ruggieri, Phys. Rev. D **77**, 054023 (2008).
[22] S. K. Ghosh, T. K. Mukherjee, M. G. Mustafa, and R. Ray, Phys. Rev **D 73**, 114007 (2006).
[23] S. K. Ghosh, T. K. Mukherjee, M. G. Mustafa, and R. Ray, Phys. Rev **D 77**, 094024 (2008).
[24] P. Deb, A. Bhattacharyya, S. Datta and S. K. Ghosh, Phys. Rev. **C 79**, 055208 (2009).
[25] A. A. Osipov, B. Hiller, J. da Providencia, Phys. Lett. **B 634**, 48-54, (2006).
[26] A. A. Osipov, B. Hiller, V. Bernard and A. H. Blin, Annals of Physics **321**, 2504-2534, (2006).
[27] A. A. Osipov, B. Hiller, A . H. Blin and J. da Providencia, Annals of Physics **322**, 2021-2054, (2007).
[28] B. Hiller, J. Moreira, A. A. Osipov and A. H. Blin, Phys. Rev. **D 81**, 116005, (2010).
[29] K. Kashiwa, H. Kouno, T. Sakagauchi, M. Matsuzaki and M. Yahiro, Phys. Lett. **B 647**, 446-451, (2007).
[30] K. Kashiwa, H. Kouno, M. Matsuzaki and M. Yahiro, Phys. Lett. **B 662**, 26-32, (2008).
[31] A. Bhattacharyya, P. Deb, S. K. Ghosh and R. Ray, Phys. Rev. **D 82**, 014021 (2010)
[32] S. A. Gottlieb *et al.*, Phys. Rev Lett. **59**, 2247 (1987).
[33] R. V. Gavai, S. Gupta and P. Majumdar, Phys. Rev. **D 65**, 054506 (2002).
[34] C. Bernard *et al.*, Phys. Rev. **D 71**, 034504 (2005).
[35] C. Bernard *et al.*, Phys. Rev. **D 77**, 014503 (2008).
[36] S. Ejiri, F. Karsch and K. Redlich, Phys. Lett. **B 633**, 275 (2006).
[37] S. Roessner, C. Ratti and W. Weise, Phys. Rev. **D 75**, 034007, (2007).
[38] C. Sasaki, B. Friman and K. Redlich, Phys. Rev. **D 75**, 074013, (2007).
[39] S. Mukherjee, M. G. Mustafa and R. Ray, Phys. Rev. **D 75**, 094015 (2007).
[40] C. Ratti, S. Roessner and W. Weise, Phys. Lett. **B 649**, 57-60, (2007).
[41] K. Fukushima, Phys. Rev. **D 79**, 074015, (2009).
[42] M. Cheng *et al.*, Phys. Rev. **D 77**, 014511, (2008).
[43] M. Cheng *et al.*, Phys. Rev. **D 79**, 074505, (2009).
[44] Borsanyi. S *et al.*, hep-lat/1007.2580v1.
[45] W. J. Fu, Y. X. Liu and Y. L. Wu, Phys. Rev. **D 81**, 014028, (2010).
[46] B. J. Schaefer and J. Wambach, Phys. Rev. **D 75**, 085015, (2007).
[47] B. J. Schaefer, J. M. Pawlowski and J. Wambach, Phys. Rev. **D 76**, 074023, (2007).
[48] B. J. Schaefer, M. Wagner and J. Wambach, Phys. Rev. **D 81**, 074013, (2010).
[49] J. Wambach, B. J. Schaefer and M. Wagner, Acta Phys. Polon. Supp. **3** 691, 2010.
[50] V. Skokov, B. Friman, E. Nakano, K. Redlich and B. J. Schaefer, Phys. Rev. **D 82** 034029 (2010).
[51] L. Stodolsky, Phys. Rev. Lett. **75**, 1044 (1995).
[52] R. Korus *et al.*, Phys. Rev. **C 64**, 054908 (2001).
[53] H. Sorge, Phys. Rev. Lett. **82**, 2048 (1999).
[54] P. F. Kolb *et al.*, Phys. Lett. **B 459**, 667 (1999).
[55] G. Boyd *et al.*, Nucl. Phys. **B 69**, 419 (1996).
[56] Y. Aoki, Z. Fodor, S. D. Katz and K. K. Szabo, JHEP, **0601**, 089 (2006).
[57] http://www.gnuplot.info/.